

The gravitating σ model in 2+1 dimensions: black hole solutions

G. Clément¹ and A. Fabbri²

Laboratoire de Gravitation et Cosmologie Relativistes

Université Pierre et Marie Curie, CNRS/ESA 7065

Tour 22/12, Boîte 142 - 4, Place Jussieu - 75252 Paris Cedex 05 - France

Abstract

We derive and discuss black-hole solutions to the gravitating $O(3)$ σ model in (2+1) dimensions. Three different kinds of static black holes are found. One of these resembles the static BTZ black hole, another is completely free of singularities, and the last type has the same Penrose diagram as the (3+1)-dimensional Schwarzschild black hole. We also construct static and dynamical multi-black hole systems.

April 1998

¹ E-mail: gecl@ccr.jussieu.fr

² Present address: Department of Physics, Stanford University, Stanford CA 94305-4060, USA;
E-mail: afabbri1@leland.stanford.edu

1. Introduction

Models in lower-dimensional gravity are useful as laboratories where we can study analytically situations which can often be addressed only numerically in the full four-dimensional setting. A great impetus in the study of (2+1)-dimensional gravity came from the discovery [1] of black-hole solutions to cosmological gravity with $\Lambda < 0$ [2]. Less well known is the existence of black-hole solutions to the coupled Einstein-Maxwell equations with a negative gravitational constant, first pointed out by Kogan [3].

Another model which lends itself to the analytical construction of stationary solutions is the (2+1)-dimensional gravitating $O(3)$ σ model. The reason is that this model admits stationary multi-soliton solutions classified by an integer winding number. The flat-space soliton or vortex solutions originally given by Belavin and Polyakov [4] were first generalized to self-gravitating soliton solutions by Clément [5], and independently by Comtet and Gibbons [6]. Wormhole solutions to this model were discussed in [7]. The aim of the present work is to derive and discuss black-hole and multi-black hole solutions to the gravitating σ model.

This model is presented in the next section. We show that the coupled Einstein- σ field equations in three dimensions may be obtained, for a special (negative) value of the gravitational constant, by dimensional reduction from a sector of the stationary Einstein-Maxwell equations in (3+1) dimensions. We then show that a subset of solutions to the (2+1)-dimensional Einstein- σ theory, depending on a single real potential, are in one-to-one correspondence with solutions to the (2+1)-dimensional Einstein-Maxwell theory.

In Sect. 3 we discuss static and stationary solutions to the (2+1)-dimensional Einstein- σ theory. A first set of static solutions are the multi-soliton solutions of [5],[6],[7]. We are concerned in the present paper with a second set of solutions, which we construct explicitly in the case of rotationally symmetric fields depending on a single real potential. We also discuss briefly the extension of these static solutions to stationary solutions of the (2+1)-dimensional Einstein- σ equations and, in an Appendix, their extension to stationary solutions of the (3+1)-dimensional Einstein-Maxwell equations.

Sect. 4 is devoted to the study of the causal structure of the two classes of static circularly symmetric solutions constructed in Sect. 3. The solutions of the first class generically have a non-analytical singularity. However we show that for negative values of the gravitational constant these solutions may be analytically extended, for an infinite set of discrete values of an integration constant, to black-hole spacetimes falling in two subclasses. The black holes of the first subclass have a Penrose diagram similar to that

of a static BTZ black hole, with a spacelike singularity hidden behind the horizon. The spacetimes of the second subclass are completely regular, with a Penrose diagram similar to that of the extreme BTZ black hole. Finally, the solutions of the second class may also be extended to black holes for negative values of the gravitational constant, with a Penrose diagram similar to that of the (3+1)–dimensional Schwarzschild spacetime.

The extension of these rotationally symmetric solutions to multicenter solutions is discussed in Sect. 5. These multi–black hole solutions generically admit conical singularities. The requirement that the conical singularities follow geodesics leads to two possibilities. The first is that the solution is time–independent, with the conical singularities lying on the horizon(s). The second possibility is that of an explicitly time–dependent solution describing a dynamical system of freely falling black holes and conical singularities. We discuss briefly the dynamical evolution of such two-black hole systems for the three different black hole species described in Sect. 4.

2. The three–dimensional gravitating $O(3)$ non–linear σ model and its one–potential sector

The three–dimensional $O(3)$ non–linear σ model coupled to gravity is defined by the action

$$S = \frac{1}{2} \int d^3x \sqrt{|g|} \left[-\frac{1}{\kappa} g^{\mu\nu} R_{\mu\nu} + g^{\mu\nu} \partial_\mu \vec{\phi} \partial_\nu \vec{\phi} + \lambda(\vec{\phi}^2 - \nu^2) \right], \quad (2.1)$$

where $\kappa = 8\pi G_3$, and the Lagrange multiplier λ constrains the isovector field $\vec{\phi}$ to vary on the two-sphere $\vec{\phi}^2 = \nu^2$. Following [7] we construct the stereographic map

$$\phi_1 + i\phi_2 = \frac{2\nu\psi}{1 + |\psi|^2}, \quad \phi_3 = \nu \frac{1 - |\psi|^2}{1 + |\psi|^2}, \quad (2.2)$$

that projects the sphere $\vec{\phi}^2 = \nu^2$ on the complex ψ plane. The resulting field equations are

$$\nabla^2 \psi = \frac{2\psi^* (\nabla\psi)^2}{1 + |\psi|^2}, \quad (2.3)$$

$$R_{\mu\nu} = 2\kappa\nu^2 \frac{(\partial_\mu \psi^* \partial_\nu \psi + \partial_\nu \psi^* \partial_\mu \psi)}{(1 + |\psi|^2)^2}. \quad (2.4)$$

As we now show, these equations are in close correspondence with the stationary Einstein–Maxwell equations in (3+1) dimensions. Under the assumption of a timelike

Killing vector field ∂_t , the four-metric and the electromagnetic field may be parametrized by

$$ds_{(4)}^2 = f(dt - \omega_m dx^m)^2 - f^{-1} \gamma_{mn} dx^m dx^n \quad (2.5)$$

$$F_{m0}^{(4)} = \partial_m v, \quad F_{(4)}^{mn} = f \gamma^{-1/2} \epsilon^{mnp} \partial_p u, \quad (2.6)$$

where the various fields depend only on the spatial coordinates x^m ($m = 1, 2, 3$). The complex Ernst potentials are defined as usual by [8],[9]

$$\mathcal{E} = f - |\Phi|^2 + i\chi, \quad \Phi = v + iu, \quad (2.7)$$

where

$$\partial_m \chi = -f^2 \gamma^{-1/2} \gamma_{mn} \epsilon^{npq} \partial_p \omega_q + 2(u \partial_m v - v \partial_m u). \quad (2.8)$$

The stationary four-dimensional Einstein-Maxwell equations then reduce to the three-dimensional Ernst equations [9]

$$(\text{Re } \mathcal{E} + |\Phi|^2) \nabla^2 \mathcal{E} = (\nabla \mathcal{E} + 2\Phi^* \nabla \Phi) \nabla \mathcal{E}, \quad (2.9)$$

$$(\text{Re } \mathcal{E} + |\Phi|^2) \nabla^2 \Phi = (\nabla \mathcal{E} + 2\Phi^* \nabla \Phi) \nabla \Phi, \quad (2.10)$$

$$f^2 R_{mn}(\gamma) = \text{Re} \left[\frac{1}{2} \mathcal{E}_{,(m} \mathcal{E}^*_{,n)} + 2\Phi \mathcal{E}_{,(m} \Phi^*_{,n)} - 2\mathcal{E} \Phi_{,(m} \Phi^*_{,n)} \right], \quad (2.11)$$

where the indices m, n , as well as ∇ and ∇^2 , refer to the three metric γ_{mn} . These equations have been shown to be those of an $SU(2,1)$ σ model coupled to three-dimensional gravity [10]. The particular solution $\Phi = 0$ of Eq. (2.10) (stationary vacuum Einstein equations) reduces the system (2.9)–(2.11) to the Euclidean field equations for an $SU(1,1)$ σ model coupled to three-dimensional gravity [8]. Similarly, the particular solution [11]

$$\mathcal{E} = p^2 \quad (2.12)$$

(p real constant) of Eq. (2.9) reduces the system (2.9)–(2.11) to the Euclidean $SU(2) \sim O(3)$ σ -model field equations (2.3) and (2.4) provided we make the identifications

$$\Phi = p\psi, \quad \gamma_{mn} = g_{mn}, \quad \kappa \nu^2 = -1/2. \quad (2.13)$$

The three-dimensional gravitational constant G_3 is then negative, which is perfectly legitimate: because three-dimensional gravity is dynamically trivial, the sign of G_3 is not fixed a priori [12].

Let us also recall that the equations of the stationary Kaluza–Klein theory, i.e. five–dimensional general relativity with two Killing vectors, one timelike (∂_t) and one spacelike (∂_5) reduce, for a special ansatz, to the three–dimensional O(3) σ –model field equations (2.3) and (2.4) for $\kappa\nu^2 = -2$ [13]. One may wonder whether such a reduction also exists in the case of Einstein–Maxwell–dilaton theory

$$S = \frac{1}{16\pi} \int d^4x \sqrt{|g_4|} [-R + 2\partial^\mu\phi\partial_\mu\phi - e^{-2\alpha\phi}F^{\mu\nu}F_{\mu\nu}] \quad (2.14)$$

(ϕ is the dilaton field with coupling constant α) which interpolates between the Einstein–Maxwell theory (for $\alpha = 0$) and the Kaluza–Klein theory (for $\alpha = \sqrt{3}$). However inspection of the five–dimensional Killing algebra of the space of stationary solutions to Einstein–Maxwell–dilaton theory for $\alpha \neq 0, \sqrt{3}$ [14] shows that it does not admit an O(3) subalgebra.

A simple class of solutions to the three–dimensional sigma model (2.1) are those depending on a single real potential σ . Then general arguments [15] show that this potential can always be chosen to be harmonic,

$$\nabla^2\sigma = 0, \quad (2.15)$$

and that the fields $\vec{\phi}$ or ψ follow geodesics in target space, i.e. large circles on the sphere $\vec{\phi}^2 = \nu^2$ parametrized by the angle σ . Two examples of such large circles are the meridians

$$\vec{\phi} = (\nu \cos \alpha \sin \sigma, \nu \sin \alpha \sin \sigma, \nu \cos \sigma), \quad \psi = e^{i\alpha} \tan \frac{\sigma}{2} \quad (2.16)$$

(α constant) and the equator

$$\vec{\phi} = (\nu \cos \sigma, \nu \sin \sigma, 0), \quad \psi = e^{i\sigma}. \quad (2.17)$$

For all these large circles the Einstein equations (2.4) reduce to

$$R_{\mu\nu} = \kappa\nu^2\partial_\mu\sigma\partial_\nu\sigma. \quad (2.18)$$

Equations (2.15) and (2.18) are the field equations for a massless scalar field coupled to three–dimensional gravity or, equivalently, for Einstein–Maxwell theory in three dimensions. Indeed, the second group of Maxwell equations $F^{\mu\nu}{}_{;\nu} = 0$ implies that the dual $B_\rho \equiv \sqrt{|g|}\epsilon_{\mu\nu\rho}F^{\mu\nu}$ is a gradient, $B_\rho = \nu\partial_\rho\sigma$, i.e.

$$F^{\mu\nu} = \frac{\nu}{\sqrt{|g|}}\epsilon^{\mu\nu\lambda}\partial_\lambda\sigma. \quad (2.19)$$

The first group of Maxwell equations then gives the harmonicity condition (2.15), while the Einstein equations for the electromagnetic field give the Einstein–scalar equations (2.18), owing to the identity between the energy momentum tensors

$$T_{\mu\nu} = -F_{\mu\rho}F_{\nu}^{\rho} + \frac{1}{4}g_{\mu\nu}F_{\rho\lambda}F^{\rho\lambda} = \nu^2[\sigma_{,\mu}\sigma_{,\nu} - \frac{1}{2}g_{\mu\nu}\sigma_{,\rho}\sigma^{,\rho}]. \quad (2.20)$$

It follows that all the known solutions of the Einstein–Maxwell equations in $(2 + 1)$ dimensions [16][17][18][3][19] lead to solutions of the Einstein– σ equations (2.3) and (2.4) (however the interpretation may be somewhat different), and so also (for $\kappa\nu^2 = -1/2$) to solutions of the (3+1)–dimensional Einstein–Maxwell equations with $\mathcal{E} = p^2$, i.e. $f = p^2(1 + |\psi|^2)$, $\chi = 0$. In the case of the “meridian” ansatz (2.16), the resulting $p = 1$ four–dimensional metric

$$ds_{(4)}^2 = \frac{1}{\cos^2(\sigma/2)}dt^2 - \cos^2(\sigma/2)\gamma_{mn}dx^m dx^n \quad (2.21)$$

is singular for $\sigma = \pi \pmod{2\pi}$; the spatial sections of these spacetimes are thus generically compact with two symmetrical singularities $\sigma = \pm\pi$. The other possible large circle ansatz lead to non–static solutions. In the case of the “equator” ansatz (2.17) with $p = 1/\sqrt{2}$, we obtain

$$ds_{(4)}^2 = (dt - \omega_m dx^m)^2 - \gamma_{mn}dx^m dx^n \quad (2.22)$$

where, from Eq.(2.8), the (3+1)–dimensional gravimagnetic field

$$\partial_m\omega_n - \partial_n\omega_m = \nu^{-1}F_{mn} \quad (2.23)$$

is proportional to the (2+1)–dimensional electromagnetic field (2.19).

3. Static and stationary circularly symmetric solutions

The line element of a static (2+1)–dimensional spacetime may always be parametrized in the form

$$ds^2 = h^2 dt^2 - e^{2u}(dx^2 + dy^2). \quad (3.1)$$

where the fields h , u are time–independent. We also assume the complex scalar field ψ to be time–independent (the possibility of a time–dependent ψ shall be investigated at the

end of this section). Then, choosing complex spatial coordinates ζ , ζ^* , with $\zeta \equiv x + iy$, the Einstein equations (2.4) read [7]

$$\frac{\partial^2 h}{\partial \zeta \partial \zeta^*} = 0, \quad (3.2)$$

$$\frac{\partial^2 u}{\partial \zeta \partial \zeta^*} = -\frac{\kappa \nu^2}{(1 + |\psi|^2)^2} \left(\left| \frac{\partial \psi}{\partial \zeta} \right|^2 + \left| \frac{\partial \psi}{\partial \zeta^*} \right|^2 \right), \quad (3.3)$$

$$\frac{\partial}{\partial \zeta} \left(e^{-2u} \frac{\partial h}{\partial \zeta} \right) = -\frac{4\kappa \nu^2 h e^{-2u}}{(1 + |\psi|^2)^2} \frac{\partial \psi^*}{\partial \zeta} \frac{\partial \psi}{\partial \zeta}. \quad (3.4)$$

The general solution to Eq. (3.2) is

$$h = \text{Re } w(\zeta) \quad (3.5)$$

for some analytical function $w(\zeta)$. The case where the function $w(\zeta)$ is constant, i.e.

$$h = 1, \quad (3.6)$$

was previously treated in [5], [7], and independently in [6]. In this case Eq. (3.4) shows that ψ is an analytic (or antianalytic) function of ζ , which also solves Eq. (2.3). The integration of Eq. (3.3) then leads to two classes of multi-soliton solutions, such that the map $\psi(\zeta)$ covers an integer number of times the sphere $\vec{\phi}^2 = \nu^2$. The solutions of the first class are everywhere regular and asymptotic to the multiconical solutions of vacuum three-dimensional gravity [5], the conical singularities of the vacuum metric (δ -function sources) being smoothed out by the extended σ -model sources; the corresponding solutions of the (3+1)-dimensional Einstein equations with $\mathcal{E} = 1$ are pp -waves (see the Appendix). The solutions of the second class are also regular for $\kappa < 0$, but now they have two asymptotically conical regions at spatial infinity connected by n wormholes [7]. For $\kappa = 0$, both classes of solutions reduce to the (2+1)-dimensional static multiconical spacetime.

We are interested in this paper in the case where $w(\zeta)$ is not constant. The zeroes of this function —Killing horizons— will lead to event horizons of the metric (3.1) if the spatial metric is regular there. In particular the circularly symmetric solution must be such that the functions h and u depend only on the radial coordinate, which we may choose to be x (y is then the angular coordinate). Then the harmonic function h is

$$h = x \quad (3.7)$$

($w = \zeta$; we have absorbed an arbitrary multiplicative constant in a time rescaling). From this special choice, the general static solution with non-constant $w(\zeta)$ may be recovered by a conformal transformation, see Sect. 5. Carrying out on the static (2+1)-dimensional metric (3.1) with $h = x$ the (locally trivial) coordinate relabellings $x \rightarrow \rho$, $y \rightarrow z$ and the Wick rotation $t \rightarrow i\varphi$, and inserting the result in (2.5), we obtain (up to a gauge transformation) the (3+1)-dimensional metric

$$ds_{(4)}^2 = f(dt - \omega_3 d\varphi)^2 - f^{-1}(e^{2u}(d\rho^2 + dz^2) + \rho^2 d\varphi^2) \quad (3.8)$$

(with f and ω_3 given by (2.7) and (2.8) for $\mathcal{E} = p^2$), which is the Weyl form of the stationary axisymmetric metric if φ is an angle. Thus, the static solutions of the three-dimensional Einstein- σ equations with $\kappa\nu^2 = -1/2$ are in correspondence with stationary axisymmetric solutions of the four-dimensional Einstein-Maxwell equations with $\mathcal{E} = p^2$.

To solve the remaining (2+1)-dimensional Einstein equations, we further assume that the σ -model field depends on a single real potential σ , so that Eqs. (2.3) and (3.4) reduce to

$$h^{-1}\partial_i(h\partial_i\sigma) = 0, \quad (3.9)$$

$$\partial_\zeta(e^{-2u}\partial_\zeta h) = -\kappa\nu^2 h e^{-2u}(\partial_\zeta\sigma)^2 \quad (3.10)$$

($i = 1, 2$). Because h and u depend only on x , the left-hand side of Eq. (3.10) is real. The reality of the right-hand side then implies

$$\partial_x\sigma\partial_y\sigma = 0, \quad (3.11)$$

which has only two independent solutions, further restricted by Eq. (3.9).

The first solution $\sigma = \sigma(x)$ yields

$$\sigma = a \ln x. \quad (3.12)$$

This massless scalar field is generated by a δ -function source, so that the equivalence (2.19) with three-dimensional Einstein-Maxwell theory breaks down, as the integrability condition (2.15) is not identically satisfied. The corresponding σ -model field winds indefinitely around a large circle of the two-sphere $\vec{\phi}^2 = \nu^2$. The resulting solution to Eq. (3.10)

$$u = \frac{\kappa\nu^2 a^2}{2} \ln x + \ln b \quad (3.13)$$

leads to the spacetime metric

$$ds^2 = x^2 dt^2 - b^2 x^{\kappa\nu^2 a^2} (dx^2 + dy^2) \quad (3.14)$$

(previously given, in a different parametrization, in [20]). The only non-vanishing mixed component of the Ricci tensor is, from Eq. (2.18),

$$R_1^1 = -\kappa\nu^2 a^2 b^{-2} x^{-\kappa\nu^2 a^2 - 2} \quad (3.15)$$

so that there is generically a naked curvature singularity. The Killing horizon $x = 0$ is at infinite geodesic distance for $\kappa\nu^2 a^2 \leq -4$ while, owing to the non-analytical behavior near $x = 0$, geodesics generically terminate there for $\kappa\nu^2 a^2 > -4$. However, as we shall show in the next section, the spacetime (3.14) presents regular horizons for an infinite discrete set of values of the integration constant a .

Now we turn to the second solution of Eq. (3.11), $\sigma = \sigma(y)$. From Eq. (3.9) this results in

$$\sigma = ny. \quad (3.16)$$

Remembering that y is an angular coordinate, we see that the σ -model field $\psi(\zeta)$ is single-valued if n is integer. Integration of Eq. (3.10) then gives

$$u = -\frac{\kappa n^2 \nu^2}{4} x^2 + \ln b, \quad (3.17)$$

leading to the spacetime metric

$$ds^2 = x^2 dt^2 - b^2 e^{-\kappa n^2 \nu^2 x^2 / 2} (dx^2 + dy^2). \quad (3.18)$$

The associated solution of three-dimensional Einstein-Maxwell theory, with a radial electrostatic field $F_{01} = -bn\nu x$ corresponding to the electric charge

$$Q = \frac{1}{2} \oint \sqrt{|g|} F^{\mu\nu} \epsilon_{\mu\nu\lambda} dx^\lambda = \nu \oint d\sigma = 2\pi n\nu, \quad (3.19)$$

was previously given in [16] [17] [18] [21] [3] [19]. As we shall recall in the next section, for $\kappa < 0$ the spacetime (3.18) is a black hole with a Penrose diagram similar to that of the Schwarzschild solution [3]. Let us also note that when κ goes to zero both metrics (3.14) and (3.18) go over into the rotationally symmetric Rindler metric

$$ds^2 = x^2 dt^2 - dx^2 - dy^2. \quad (3.20)$$

We shall not attempt here a full investigation of the stationary problem associated with the action (2.1). As in the (2+1)–dimensional Einstein–Maxwell case [16], a subset of rotating solutions may be generated from the static circularly symmetric solutions given above by the local coordinate transformation

$$t \rightarrow t - \omega y \tag{3.21}$$

(ω constant). While the corresponding local transformation on the (3+1)–dimensional stationary axisymmetric metric (3.8) $\varphi \rightarrow \varphi - \gamma z$ is innocuous, the transformation (3.21) may lead to the appearance of closed timelike curves, because of the periodicity of y . The resulting stationary solutions are discussed in the next section.

Other stationary solutions to the Einstein– σ model may be obtained by relaxing the assumption that the complex field ψ is time–independent to allow for fields ψ depending periodically on time. We again assume that ψ depends on a single real potential σ and that the spacetime metric is static. Then, the $(0, i)$ component of Eq. (2.18) gives

$$\partial_t \sigma \partial_i \sigma = 0, \tag{3.22}$$

so that if σ is time–dependent then it must be space–independent and, from Eq. (2.15), linear in time,

$$\sigma = ct, \tag{3.23}$$

which indeed corresponds to a periodic σ –model field. Note that the field (3.23) is obtained from (3.16) by the interchange $y \leftrightarrow t$. It follows that the same interchange, accompanied by the continuation $x^2 \rightarrow -x^2$ and $b^2 \rightarrow -b^2$ so that the new metric has the correct signature, leads to the static circularly symmetric metric generated by (3.23)

$$ds^2 = b^2 e^{\kappa c^2 \nu^2 x^2 / 2} (dt^2 - dx^2) - x^2 dy^2. \tag{3.24}$$

The associated “magnetic” solution of three–dimensional Einstein–Maxwell theory, with a radial magnetic field $F_{12} = bc\nu x$, was first given by Melvin [18] (see also [3] [19]). The metric (3.24) is regular for $\kappa > 0$ if $b = 1$, and singular, with compact spatial sections, for $\kappa < 0$. Other stationary solutions (previously given in the Einstein–Maxwell case in [19]) may be generated from (3.23) (3.24) by the local coordinate transformation (3.21), which leads to single–valued σ –model fields only for the discrete values $\omega_n = n/c$.

4. Analysis of the global causal structure of these solutions

In this section we study the causal structure of the static spacetimes (3.14) and (3.18), as well as of their stationary extensions by the local transformation (3.21). We first consider the spacetime metric (3.14), which can be transformed to the conformal gauge metric

$$ds^2 = \left(\frac{|\alpha|}{b} r \right)^{2/\alpha} (dt^2 - dr^2) - \alpha^2 r^2 dy^2, \quad (4.1)$$

by the coordinate transformation $r = (b/|\alpha|)x^\alpha$, where we have put $\alpha \equiv \kappa\nu^2 a^2/2 \neq 0$. The resulting Penrose diagram is a triangle bounded by the spacelike side $r = 0$ and the two lightlike sides $r \pm t = \infty$. To further elucidate the conformal structure of this family of spacetimes, we transform for $\alpha \neq -2$ to the new radial coordinate $\rho = bx^{\alpha+2}/|\alpha+2|$, leading to the Schwarzschild-like form of this solution

$$ds^2 = f dt^2 - \frac{1}{f} d\rho^2 - b^2 f^\alpha dy^2, \quad (4.2)$$

with

$$f(\rho) = \left(\frac{|\alpha+2|}{b} \rho \right)^{2/(\alpha+2)} \quad (4.3)$$

(the case $\alpha = -2$, i.e. $\kappa\nu^2 a^2 = -4$, shall be considered below, Eq. (4.10)).

The metric (4.2) is generically singular for $\rho = 0$, that is $r = 0$ for $\alpha < -2$ or $\alpha > 0$, and $r = \infty$ for $-2 < \alpha < 0$; the Penrose diagrams for the three cases $\alpha < -2$, $-2 < \alpha < 0$, and $\alpha > 0$ are shown in Figs. 1, 2 and 4. The Killing horizon corresponds to $\rho = 0$ for $\alpha > -2$, and to $\rho = \infty$ ($r = \infty$) for $\alpha < -2$, in which case it is at infinite geodesic distance. So the Killing horizon is lightlike and at finite geodesic distance only for $-2 < \alpha < 0$. For $-1 < \alpha < 0$, the curvature scalar (3.15) diverges on this horizon. For $-2 < \alpha < -1$, the curvature scalar vanishes on the horizon; nevertheless, geodesics generically cannot be extended beyond it because of the non-analytical behaviour of the function $f(\rho)$. However, for

$$\alpha = \frac{2(1-n)}{n} \quad (4.4)$$

(n integer), $f(\rho) \propto \rho^n$ is analytical and the spacetime can be extended. To check this we study the geodesic equation which can be integrated, using the two constants of the motion (energy and angular momentum)

$$f \dot{t} = E, \quad b^2 f^\alpha \dot{y} = L, \quad (4.5)$$

to

$$\dot{\rho}^2 - E^2 + \frac{L^2}{b^2} f^{1-\alpha} + \varepsilon f = 0, \quad (4.6)$$

where a dot means derivative with respect to an affine parameter, and $\varepsilon = +1, 0$ or -1 for timelike, lightlike or spacelike geodesics. For the discrete set of values (4.4) of the constant α , both f and $f^{1-\alpha} \propto \rho^{3n-2}$ are analytical so that the geodesics can be extended beyond $\rho = 0$ by changing ρ to $-\rho$.

The case $n = 1$ ($\alpha = 0$) corresponds to the rotationally symmetric Rindler metric (3.20) which, as is well known, is regular and admits the cylindrical Minkowski spacetime (with cylindrical spatial sections) as its maximal extension (Fig. 3). All other values of $n > 1$ correspond to degenerate horizons. For n odd, $n = 3, 5, \dots$, the Killing field ∂_t becomes spacelike in the sector II ($\rho < 0$), where the geodesic equation becomes

$$\dot{\rho}^2 - E^2 - \frac{L^2}{b^2} |f|^{1-\alpha} - \varepsilon |f| = 0, \quad (4.7)$$

showing that geodesics terminate at the spacelike point singularity $\rho \rightarrow -\infty$ ($|f| \rightarrow \infty$). The Penrose diagram of the resulting maximal extension, shown in Fig. 5, is similar to that of the static BTZ black hole [1] (except that the spacelike singularity of the BTZ black hole is not a curvature singularity, but a singularity in the causal structure). An important difference is that, in the present case, the circle at spacelike infinity ($\rho \rightarrow +\infty$) is actually a point, the lengths of concentric circles around this increasing with decreasing “radius” ρ as ρ^{1-n} , so that the length of the event horizon $\rho = 0$ is infinite. The vanishing of the surface gravity at this horizon also implies that the associated Hawking temperature is zero (such “cold black holes”, obeying a similar quantization property, have also been found as solutions to scalar–tensor theories [22]). From Eq. (4.6), almost all geodesics (all except spacelike geodesics with $E = 0$) cross this horizon to fall towards the singularity $\rho \rightarrow -\infty$.

For n even, $n = 2, 4, \dots$, $\rho = 0$ is a horizon of even order connecting two isometrical sectors I ($\rho > 0$) and I' ($\rho < 0$) where the Killing field ∂_t is timelike. As before, this horizon has infinite proper length and is crossed by almost all geodesics. The maximal extension is a geodesically complete infinite sequence of sectors I and I', leading to a Penrose diagram (Fig. 6), which is similar to the Penrose diagram for the extreme BTZ black hole $J = Ml$ [1] and its $M \rightarrow 0$ limit, the BTZ “vacuum” solution

$$ds^2 = \frac{r^2}{l^2} dt^2 - \frac{l^2}{r^2} dr^2 - r^2 d\varphi^2. \quad (4.8)$$

Again, we must keep in mind that in our case the circles at infinity $\rho \rightarrow \pm\infty$ are contracted to points. The similarity —and the difference— with the BTZ vacuum solution (4.8) is most obvious in the special case $n = 2$ ($\alpha = -1$, i.e. $\kappa\nu^2 a^2 = -2$) where $\rho = bx$ and our metric (3.14) takes the form

$$ds^2 = x^2 dt^2 - b^2 x^{-2} dx^2 - b^2 x^{-2} dy^2. \quad (4.9)$$

In the limit $n \rightarrow \infty$, Eq. (4.4) goes over into $\alpha = -2$ ($\kappa\nu^2 a^2 = -4$). The Schwarzschild form of the metric (3.14) is in this case (4.2) with

$$f(\rho) = e^{-2\rho/b} \quad (4.10)$$

($\rho = -b \ln x$). The Penrose diagram is the same as for $\alpha < -2$ (Fig. 1). The Killing horizon $\rho \rightarrow +\infty$ is at infinite geodesic distance, while only spacelike geodesics ($\varepsilon = -1$) reach the singularity $\rho \rightarrow -\infty$, massive or massless test particles being repelled by an exponentially rising potential barrier.

Performing on (3.14) the local coordinate transformation (3.21), we obtain the stationary solution

$$ds^2 = x^2 dt^2 - 2\omega x^2 dt dy + (\omega^2 x^2 - b^2 x^{2\alpha}) dy^2 - b^2 x^{2\alpha} dx^2. \quad (4.11)$$

Invariant spacetime properties, such as the curvature scalar (3.15) or the integrated geodesic equation (4.6), being unaffected by coordinate transformations, the Penrose diagrams for the stationary spacetimes (4.11) are the same as for the corresponding static spacetime (3.14). The only new feature induced by the transformation (3.21) is the appearance of closed timelike curves (CTCs). The circles $t = \text{const.}$, $x = \text{const.}$ are CTCs for $x > x_0 \equiv (\omega/b)^{1/(\alpha-1)}$ if $\alpha < 1$, and for $x < x_0$ if $\alpha > 1$. Accordingly, CTCs occur in the region extending from the circle $\rho = \rho_0 \equiv bx_0^{\alpha+2}/|\alpha+2|$ to the singularity $\rho = 0$ if $\alpha \leq -2$ or $\alpha > 1$, and between the circle $\rho = \rho_0$ and spacelike infinity $\rho \rightarrow \infty$ for $-2 < \alpha < 1$. For $\alpha = 1$, all the circles $t = \text{const.}$, $x = \text{const.}$ are CTCs if $|\omega| > b$, and CLCs (closed lightlike curves) if $|\omega| = b$. The metrics (4.11) with $\alpha = 1$, $|\omega| < b$ do not admit CTCs, and all describe the same static spacetime, as may be shown by performing on (4.11) the global coordinate transformation

$$t = \left(1 - \frac{\omega^2}{b^2}\right)^{1/2} \hat{t}, \quad x = b^{-1} \hat{x}, \quad y = b^{-1} \left(1 - \frac{\omega^2}{b^2}\right)^{-1/2} \left(\hat{y} - \frac{\omega}{b} \hat{t}\right) \quad (4.12)$$

to the static conformally flat metric

$$ds^2 = \frac{\hat{x}^2}{b^2} (d\hat{t}^2 - d\hat{x}^2 - d\hat{y}^2). \quad (4.13)$$

Now we consider the causal structure of the second static solution, Eq. (3.18), which can be put in the Schwarzschild-like form

$$ds^2 = f dt^2 - f^{-1} d\rho^2 - \left(\frac{\kappa n^2 \nu^2}{2}\right)^2 \rho^2 dy^2 \quad (4.14)$$

with

$$f = x^2 = \frac{2}{\kappa n^2 \nu^2} (B - \ln \rho^2). \quad (4.15)$$

The constant $B \equiv 2 \ln(2b/\kappa n^2 \nu^2)$ can be identified as a mass parameter. The global causal structure of this spacetime, considered as a solution of the Einstein–Maxwell equations in (2+1) dimensions, has previously been discussed in the case $\kappa > 0$ by Gott et al. [17], and for both signs of κ by Kogan [3]. The Ricci tensor has a single nonvanishing component

$$R_2^2 = -\frac{4}{\kappa n^2 \nu^2 \rho^2}, \quad (4.16)$$

showing that $\rho = 0$ is the location of a curvature singularity, while the Killing horizon corresponds to $\rho = \rho_h \equiv e^{B/2}$. The temperature associated with this horizon is $\exp(-B/2)/(\pi|\kappa|n^2\nu^2)$ [21]. Let us first consider the case $\kappa > 0$. In the region $0 < \rho < \rho_h$, where t is a timelike coordinate, there is a timelike singularity at $\rho = 0$ where the spacetime is null, timelike and spacelike incomplete. In the region $\rho_h < \rho < \infty$, on the other hand, ρ becomes a timelike coordinate and the boundary $\rho = \infty$ is geodesically complete. Following the simple rules given in [23] we can construct the maximally extended Penrose diagram, which is represented in Fig. 7. As also suggested in [17] the singularity structure of this solution is very similar to that of the Reissner–Nordström solution and corresponds to two point charges with opposite values of the electric charge. Also, $\rho = \rho_h$ does not correspond to an event horizon, but to a Cauchy horizon similar to the inner horizon of the Reissner–Nordström solution.

We find more interesting to interpret physically the solution given by $\kappa < 0$ (as first indicated in [3]). The analysis is similar to that of the previous case, except for the important fact that the signature of the metric is changed: $\rho = 0$ is a spacelike singularity, $\rho = \rho_h$ is an event horizon and $\rho = \infty$ is still infinitely distant. The Penrose diagram is identical to that of the Schwarzschild solution, see Fig. 8 (it is obtained by rotating

the diagram of Fig. 7 by 90 degrees), and therefore this solution represents a black hole. This is probably the black hole solution of three-dimensional gravity which, at least for what concerns the causal structure, is closest to its four-dimensional version, i.e. the Schwarzschild black hole. In this case, the integrated geodesic equation reads

$$\dot{\rho}^2 + V(\rho) = E^2, \quad V(\rho) = -\frac{2}{\kappa n^2 \nu^2} (\ln \rho^2 - B) \left(\varepsilon + \frac{\lambda^2}{\rho^2} \right) \quad (4.17)$$

($\lambda = 2L/\kappa n^2 \nu^2$). The form of $V(\rho)$ depends on the value of λ . For $|\lambda| < e^{1+B/2}$, see Fig. 9, all timelike geodesics ($\varepsilon = +1$) get captured by the black hole, i.e. their worldlines start at the past singularity and end in the future singularity of Fig. 8. This peculiar behaviour, not shared by all geodesics in the Schwarzschild spacetime, is due to the fact that the static frame (t, ρ) is not asymptotically inertial, i. e. the black hole will not be seen at rest relative to an inertial observer at infinity. A similar phenomenon has been shown to exist in [24] for solutions to 1 + 1 dimensional dilaton gravity representing black holes which are static only as viewed by asymptotic accelerated (Rindler) observers. In the case $|\lambda| > e^{1+B/2}$, on the other hand, we show in Fig. 10 that, due to the ‘high’ angular momentum, bounded motion, in particular also circular orbits, is possible.

The stationary solution generated from the static solution (4.14) by the local transformation (3.21) is

$$ds^2 = f dt^2 - 2\omega f dt dy + \left(\omega^2 f - \left(\frac{\kappa n^2 \nu^2}{2} \right)^2 \rho^2 \right) dy^2 - f^{-1} d\rho^2. \quad (4.18)$$

Again, the global causal structure of these stationary spacetimes is the same as that of the original static spacetime, except for the appearance of CTCs in the regions where g_{yy} may become positive. For $\kappa > 0$, g_{yy} always has a zero at some $\rho = \rho_1 < \rho_h$, and CTCs occur between the circle $\rho = \rho_1$ and the singularity at $\rho = 0$. For $\kappa < 0$, g_{yy} has a maximum at $\rho = \rho_m \equiv \omega(-\kappa n^2 \nu^2 / 2)^{-3/2}$; if $\rho_m < e^{(1+B)/2}$, g_{yy} is negative at $\rho = \rho_m$ and so everywhere outside the horizon, and there are no CTCs; if $\rho_m > e^{(1+B)/2}$, g_{yy} vanishes on two lightlike circles outside the horizon, and CTCs occur in the region between these two circles.

5. Multibody structure

The general static multicenter solution to Eqs. (3.2)-(3.4) can in principle be constructed by replacing in (3.5) the one-particle solution $w = \zeta \equiv x + iy$ (where x and y are the radial and angular coordinate respectively) by

$$w = A_0 + \sum_{i=1}^N A_i \ln(z - a_i) \quad (5.1)$$

(where now $z = e^\zeta$) for real weights A_0, A_i and complex center locations a_i . The corresponding potential σ solving Eq. (3.9) is then (up to an additive constant)

$$\sigma_{(1)} = a \ln \operatorname{Re} w(z) \quad (5.2)$$

for the first class of solutions, and

$$\sigma_{(2)} = c \operatorname{Im} w(z) \quad (5.3)$$

for the second class. In this last case, the resulting σ -model field $\psi(z)$ is single-valued only if all the cA_i are integers,

$$A_i = \frac{n_i}{c}. \quad (5.4)$$

The metric function u in (3.1) is then obtained by integrating Eq. (3.10), which may be written as

$$\partial_z u = \frac{1}{2} \partial_z \ln(\partial_z w) + \kappa \nu^2 h (\partial_w \sigma)^2 \partial_z w, \quad (5.5)$$

leading to the two classes of solutions

$$ds_{(1)}^2 = h^2 dt^2 - b^2 h^{\kappa \nu^2 a^2} |w'(z)|^2 dz dz^* \quad (5.6)$$

(where $h = \operatorname{Re} w(z)$, and b is a constant), and

$$ds_{(2)}^2 = h^2 dt^2 - b^2 e^{-\kappa c^2 \nu^2 h^2 / 2} |w'(z)|^2 dz dz^*. \quad (5.7)$$

This solution describes a distribution of p black holes (where $p \leq N$ is the number of disconnected components of the horizon $h = 0$) under the same conditions as for the one-particle solutions, i.e. $\kappa \nu^2 a^2 = 4(1 - n)/n$ (n positive integer) for the first class of solutions, and $\kappa < 0$ for the black holes of the second class. However, besides the p black holes, additional conical singularities will in general be present at the $(N - 1)$ zeroes z_j of the function $w'(z)$ [25] [26]. It is in principle possible to choose the parameters in (5.1) so that these conical singularities are absent, which is the case if the parameters are constrained by the $2(N - 1)$ relations

$$\sum_{i=1}^n A_i a_i^q = 0, \quad (5.8)$$

for $q = 1, \dots, N - 2$ (i.e. all the multipole moments until the 2^{N-2} order vanish). But the function $w'(z)$ will still have a pole of order N , leading for $N > 2$ to a conical singularity

at $z \rightarrow \infty$ (but at finite geodesic distance) of the metric (5.6) or (5.7). In the case $N = 2$ the regular solution is

$$w(z) = A_0 + A_1 \ln \left(\frac{z - a_1}{z - a_2} \right); \quad (5.9)$$

the corresponding horizon

$$\frac{|z - a_1|}{|z - a_2|} = e^{-A_0/A_1} \quad (5.10)$$

being a circle, the resulting one-black hole spacetimes are identical to those of Sect. 3.

So for $N > 2$ the solutions (5.6) or (5.7) always admit conical singularities. As conical singularities correspond in $2 + 1$ gravity to point particles we will require, for consistency, that their worldlines are geodesics of the spacetime [25]. Such freely falling particles momentarily at rest ($v^i \equiv dx^i/dt = 0$) can remain at rest only if the Newtonian force

$$\frac{dv^i}{dt} = \frac{1}{2} g^{ij} \partial_j g_{00} = -e^{-2u} h \partial_i h \quad (5.11)$$

vanishes at their location. In the case of the above multi-center solutions (5.6) (5.7), this is possible only if the conical singularities lie on the horizon, i.e. if the parameters in (5.1) are constrained by the $(N - 1)$ relations

$$h(z_j) = 0. \quad (5.12)$$

The horizon world-sheet being generated by null geodesics, it follows that the conical singularities at $z = z_j$ do lie on null geodesics when the conditions (5.12) are satisfied. Under these conditions, the generic N -center solution, which has a single horizon with $(N - 1)$ self-intersections, is seen by an outside observer as a static system of N black holes and $(N - 1)$ conical singularities.

The global structure of such multi-black hole spacetimes depends on the analytical extensions which are performed. Let us discuss for definiteness the case $N = 2$, $A_1 = A_2$ (symmetrical two-black hole). In this case the horizon makes a figure 8. To each half of this 8 we can glue a distinct “interior” region II of the extended one-black hole spacetime. Then, we can glue the other horizon of each of these regions II to one of the two halves of the figure 8 horizon in an exterior two-black hole region identical to the first one. Such a symmetrical extension can easily be generalized to a N -black hole spacetime made of two identical exterior regions connected by N Einstein-Rosen-like bridges [27]. In a more economical extension ($N = 2$), similar to the Wheeler-Misner construction of [28], the two exterior regions are identified, i.e. the two horizons bounding a single interior region II

are glued to the two horizons of the same exterior region; this construction can easily be generalized to any even N , with a single interior region and $N/2$ interior regions II. In the case of the first class of black hole solutions with n even, where the one–black hole regions II are isometrical to the regions I, the simplest causal symmetrical extension is achieved, for any N , by gluing the N future horizons of an exterior region to the N past horizons of the next exterior region. The resulting generalized Penrose diagram is similar to the diagram (Fig. 6) for the one–black hole spacetime, with multiple lines at 45° standing for the multiple horizon components [26].

While consistent, such static multi–black hole solutions seem rather special, as one would intuitively expect that black holes should attract (and therefore fall on) each other. However, following [26] one can generalize these static solutions to consistent dynamical solutions of the Einstein– σ equations by taking the N complex parameters a_i in (5.1) to be time–dependent,

$$a_i = a_i(t), \tag{5.13}$$

and requiring that the $(N - 1)$ conical singularities $\zeta_j(t)$ follow geodesics of the resulting spacetime. The unknown functions $a_i(t)$ are then determined from given initial conditions, up to an arbitrariness corresponding to that of the center–of–mass motion of the system.

Let us show for definiteness how to construct such a dynamical solution corresponding to a system of two black holes with equal masses. Choose a particular geodesic $w = w_1(t)$ in a one–black hole spacetime $w = \zeta$ of Sect. 3 , and make the global coordinate transformation

$$z^2 = c[e^{w/\alpha} - e^{w_1(t)/\alpha}] \tag{5.14}$$

($c, \alpha > 0$ real constants). The time–dependent field configuration $(\sigma(z, t), g_{\mu\nu}(z, t))$ transformed from the static $N = 1$ solution $(\sigma(w), g_{\mu\nu}(w))$ by the coordinate transformation (5.14) is, by construction, a solution of the Einstein– σ equations, with the conical singularity $z = 0$ following a geodesic. This solution is of the form (5.1) with $N = 2, A_0 = -\alpha \ln c, A_1 = A_2 = \alpha, a_1(t) = -a_2(t) = \sqrt{-c} e^{w_1(t)/2\alpha}$. The static solution discussed above is recovered if we choose the special null geodesic $\varepsilon = L = E = 0$ in Eq. (4.6) or (4.17).

We briefly discuss the dynamical evolution of such two–black hole systems generated from the different types of one–black holes encountered in this paper. In the case of the first–class black holes with n odd ($n > 1$; the case $n = 1$ is treated in [26]), the consideration

of the generic timelike or null geodesic³ leads to the following picture. A distant observer sees a single past horizon suddenly developing a conical singularity and bifurcating. The two horizons then separate to a finite distance and merge again (fall back on each other) after an infinite coordinate time — but a finite proper time for the distant freely falling observer, who theoretically should see the merger at the same instant he or she crosses the resulting single future horizon into the black hole (all timelike geodesics (4.6) cross the horizon $\rho = 0$). Actually our hypothetical three-dimensional observer will not live long enough, having been stretched apart and destroyed by infinitely rising tidal forces before being able to cross this horizon of infinite length [22].

The historical picture is the same in the case of the first-class black holes with n even, $n = 2q$. However, in this case $\text{Re}(w) = x = (\rho/b)^q$ stays real when the horizon is crossed ($\rho \rightarrow -\rho$), so that one can, at least formally, analytically continue (5.14) across the horizon. For q even, $\text{Re}(w)$ does not depend on the sign of ρ , so that the dynamical evolution is the same in the sectors $\rho > 0$ and $\rho < 0$. On the other hand, for q odd, $\text{Re}(w)$ changes sign with ρ . For $\rho < 0$, the line at spacelike infinity $\rho \rightarrow -\infty$ of the one-black hole solution is mapped by (5.14) into the two lines $z_\infty(t) = \pm a_1(t)$. So in a sector $\rho < 0$ there are two regions at spacelike infinity. A distant observer in one of these regions sees a conical singularity suddenly appearing on his past horizon, which merges with the past horizon of the other region at spacelike infinity. The subsequent spacelike (or lightlike) sections of this universe are “trousers” with two legs connected (at the conical singularity) to one trunk ending on a single horizon. Finally, both the conical singularity and the observer (who is destroyed in the process) fall back on the horizon.

The case of second-class black holes differs in several respects. Observers can now cross the horizon (of finite length) unharmed. Also, distant freely falling observers can avoid altogether falling into the black hole if they have enough angular momentum. Furthermore, there are now three possible dynamical evolutions for a two-black hole system, according to the nature of the timelike or null geodesic followed by the conical singularity. The first possible evolution is similar to that described for the first-class systems, except that the two horizons never actually merge for our distant observer in stationary orbit. In the second scenario, corresponding to a class of null geodesics, the two black holes, infinitely separated at $t = -\infty$, fall upon each other at the speed of light, eventually merging at $t = +\infty$. The third possibility, corresponding to a bounded motion of the conical singularity, is that of a stationary system of two black holes orbiting around their common center of mass (the conical singularity)⁴.

³ The case where the conical singularity follows a spacelike geodesic, $\varepsilon = -1$, would lead to tachyonic two-black hole systems.

⁴ Such stationary systems of two black holes with a conical singularity also occur in the case of

6. APPENDIX

In this Appendix, we discuss briefly the extension of the various static solutions (with $\kappa\nu^2 = -1/2$) of the three-dimensional Einstein- σ equations derived in Sect. 3 to $\mathcal{E} = p^2$ solutions of the (3+1)-dimensional Einstein-Maxwell equations.

In the case $h = 1$, $\psi = \psi(\zeta)$ [7], Eq. (3.3) is solved by

$$e^{2u} = (1 + |\psi|^2)|k(\zeta)|^2, \quad (6.1)$$

where $k(\zeta)$ is an arbitrary analytical function of ζ . This function can be absorbed into a redefinition of the complex variable $\zeta = x + iy$, leading to the three-dimensional Euclidean metric

$$ds_{(3)}^2 = (1 + |\psi|^2)(dx^2 + dy^2) + dz^2. \quad (6.2)$$

The corresponding stationary four-dimensional metric solving the Einstein-Maxwell equations with $\mathcal{E} = 1$ is, from (2.5),

$$ds_{(4)}^2 = (1 + |\psi|^2)(dt - \omega_3 dz)^2 - (1 + |\psi|^2)^{-1} ds_{(3)}^2, \quad (6.3)$$

where the potential ω_3 solves Eq. (2.8) which reduces, for $\mathcal{E} = 1$ and a static three-dimensional metric, to

$$\partial_\zeta \omega_3 = h^{-1} (1 + |\psi|^2)^{-2} (\psi^* \partial_\zeta \psi - \psi \partial_\zeta \psi^*), \quad (6.4)$$

leading in the present case to

$$\omega_3 = -(1 + |\psi|^2)^{-1}. \quad (6.5)$$

We thus arrive at the four-dimensional metric

$$ds_{(4)}^2 = (1 + |\psi|^2) dt^2 + 2 dt dz - dx^2 - dy^2, \quad (6.6)$$

which corresponds to a subclass of pp -wave spacetimes [8].

In the other case treated in Sect. 3, $h = x$ and ψ is assumed to depend on a single real potential σ . As discussed at the end of Sect. 2, the corresponding four-dimensional Einstein-Maxwell solution is singular in the case of the meridian ansatz (2.16). We will

extreme BTZ black holes [26].

consider here only the case of the equator ansatz $\psi = e^{i\sigma}$ with $\mathcal{E} = 1/2$. The resulting four-dimensional metric is then (3.8) with $f = 1$ and, from Eqs. (2.19) and (2.23),

$$\partial_i \omega_3 = -\rho \epsilon_{ij} \partial_j \sigma. \quad (6.7)$$

In the case of the three-dimensional metric (3.14) with $\sigma = a \ln x$, we thus obtain the four-dimensional metric and electromagnetic potentials

$$ds_{(4)}^2 = (dt - az d\varphi)^2 - b^2 \rho^{-a^2/2} (d\rho^2 + dz^2) - \rho^2 d\varphi^2, \quad (6.8)$$

$$v = \frac{1}{\sqrt{2}} \cos(a \ln \rho), \quad u = \frac{1}{\sqrt{2}} \sin(a \ln \rho). \quad (6.9)$$

The curvature invariant $R^{\mu\nu} R_{\mu\nu} \propto \rho^{a^2-4}$ is singular at $\rho = 0$ if $|a| < 2$, and at $\rho \rightarrow \infty$ if $|a| > 2$. The case $|a| = 2$,

$$ds_{(4)}^2 = (dt - 2z d\varphi)^2 - \frac{b^2}{\rho^2} (d\rho^2 + dz^2) - \rho^2 d\varphi^2, \quad (6.10)$$

corresponds to the regular homogeneous solution of the Einstein–Maxwell equations previously obtained by McLenaghan and Tariq [29] and Tupper [30]. The axis $\rho = 0$ is at infinite geodesic distance; let us also mention that all the circles t, ρ, z constant are timelike for $4z^2 - \rho^2 > 0$.

Similarly, the three-dimensional metric (3.18) with $\sigma = -2ay$ ($a = -n/2$ real) leads to the four-dimensional metric and electromagnetic potentials

$$ds_{(4)}^2 = (dt - a\rho^2 d\varphi)^2 - b^2 e^{a^2 \rho^2} (d\rho^2 + dz^2) - \rho^2 d\varphi^2, \quad (6.11)$$

$$v = \frac{1}{\sqrt{2}} \cos(2az), \quad u = -\frac{1}{\sqrt{2}} \sin(2az), \quad (6.12)$$

previously given by McIntosh [31]. The metric (6.11) admits CTCs for $\rho > |a|^{-1}$. A common feature of the solutions (6.10) and (6.11) is that in both cases the Maxwell field does not share the spacetime symmetry [31] [8].

References

- [1] M. Bañados, C. Teitelboim and J. Zanelli, Phys. Rev. Lett. 69 (1992) 1849; M. Bañados, M. Henneaux, C. Teitelboim and J. Zanelli, Phys. Rev. D 48 (1993) 1506.
- [2] S. Carlip, Class. Quant. Grav. 12 (1995) 2853.
- [3] I.I. Kogan, Mod. Phys. Lett. A 7 (1992) 2341.
- [4] A.A. Belavin and A.M. Polyakov, JETP Lett. 22 (1975) 245.
- [5] G. Clément, Nucl. Phys. B 114 (1976) 437.
- [6] A. Comtet and G. Gibbons, Nucl. Phys. B 299 (1988) 719.
- [7] G. Clément, Phys. Rev. D 51 (1995) 6803.
- [8] D. Kramer, H. Stephani, M. MacCallum, and E. Herlt, *Exact Solutions of the Einstein Field Equations*, CUP, 1980.
- [9] F.J. Ernst, Phys. Rev. 168 (1968) 1415.
- [10] P.O. Mazur, Acta Phys. Polon. B14 (1983) 219; A. Eris, M. Gürses, and A. Karasu, J. Math. Phys. 25 (1984) 1489.
- [11] Y. Tanabe, Progr. Theor. Phys. 57 (1977) 840.
- [12] S. Deser, R. Jackiw and G. 't Hooft, Ann. Phys. (NY) 152 (1984) 220.
- [13] G. Clément, Gen. Rel. Grav. 18 (1986) 137.
- [14] D.V. Gal'tsov, A.A. Garcia and O.V. Kechkin, Class. Quant. Grav. 12 (1995) 2887.
- [15] G. Neugebauer and D. Kramer, Ann. der Physik (Leipzig) 24 (1969) 62.
- [16] S. Deser and P.O. Mazur, Class. Quant. Grav. 2 (1985) L51.
- [17] J.R. Gott, III, J.Z. Simon and M. Alpert, Gen. Rel. Grav. 18 (1985) 1019.
- [18] M.A. Melvin, Class. Quant. Grav. 3 (1986) 117.
- [19] G. Clément, Class. Quant. Grav. 10 (1993) L49.
- [20] K.S. Virbhadra, preprint gr-qc/9408035 (1994).
- [21] B. Reznik, Phys. Rev. D 45 (1992) 2151.
- [22] K.A. Bronnikov, C.P. Constantinidis, R.L. Evangelista and J.C. Fabris, preprint gr-qc/9710092; K.A. Bronnikov, G. Clément, C.P. Constantinidis and J.C. Fabris, preprint gr-qc/9801050, to be published in Phys. Lett. A .
- [23] T. Klösch and T. Strobl, Class. Quant. Grav. 13 (1996) 2395.
- [24] R. Balbinot and A. Fabbri, Class. Quant. Grav. 13 (1996) 2457.
- [25] S. Deser and R. Jackiw, Ann. Phys. (NY)153 (1984) 405.
- [26] G. Clément, Phys. Rev. D 50 (1994) R7119.
- [27] A. Einstein and N. Rosen, Phys. Rev. 48 (1935) 73.
- [28] G. Clément, J. Math. Phys. 38 (1997) 5807.
- [29] R.G. McLenaghan and N. Tariq, J. Math. Phys. 18 (1975) 2306.
- [30] B.O.J. Tupper, Gen. Rel. Grav. 7 (1976) 479.
- [31] C.B.G. McIntosh, Gen. Rel. Grav. 9 (1978) 277.

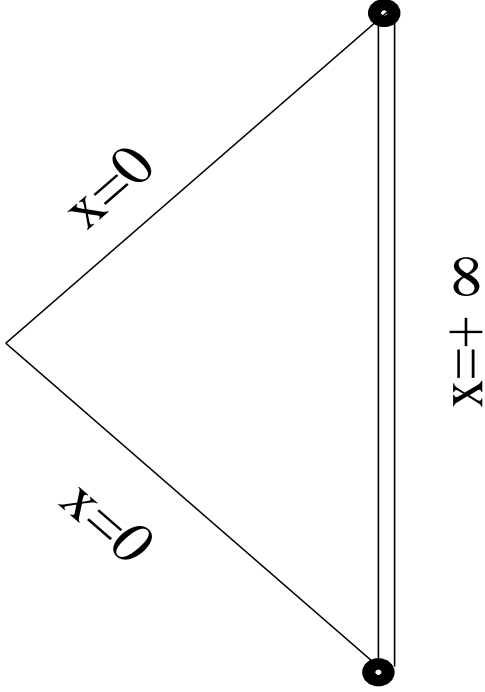


Fig. 1: Penrose diagram for the spacetime (4.2) with $\alpha \leq -2$. The radial coordinate $x = (g_{tt})^{1/2}$ is related to the coordinate ρ of (4.2) by $\rho = bx^{\alpha+2}/|\alpha + 2|$. The singularity is represented by a double line.

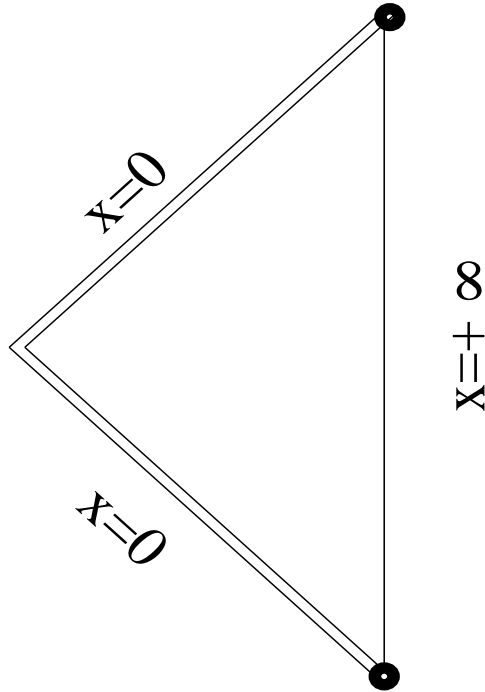


Fig. 2: Penrose diagram for the spacetime (4.2) with $-2 < \alpha < 0$.

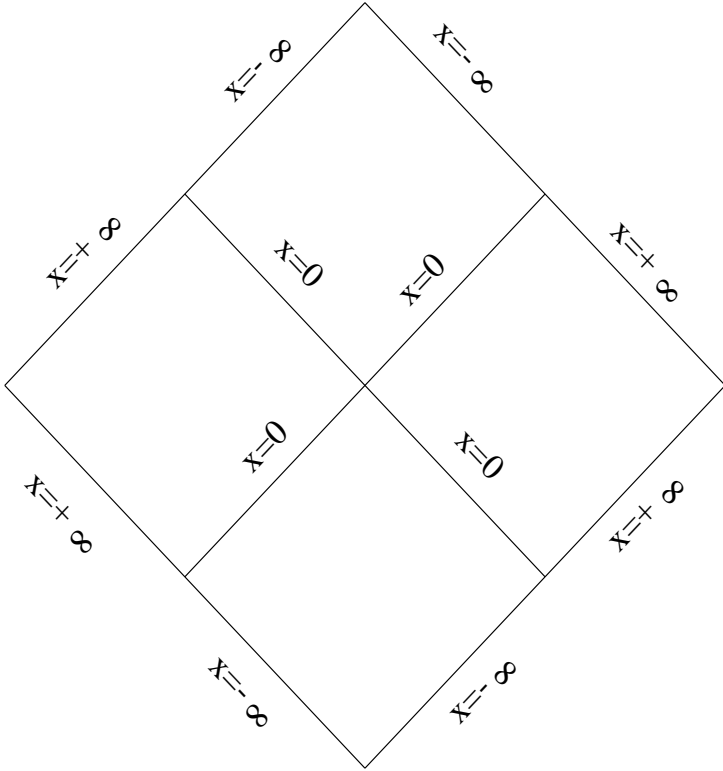


Fig. 3: Penrose diagram for the spacetime (4.2) with $\alpha = 0$.

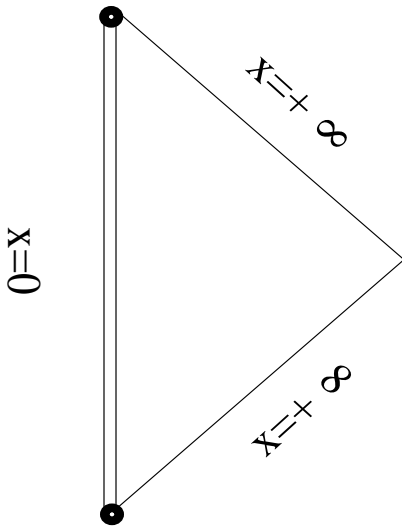


Fig. 4: Penrose diagram for the spacetime (4.2) with $\alpha > 0$.

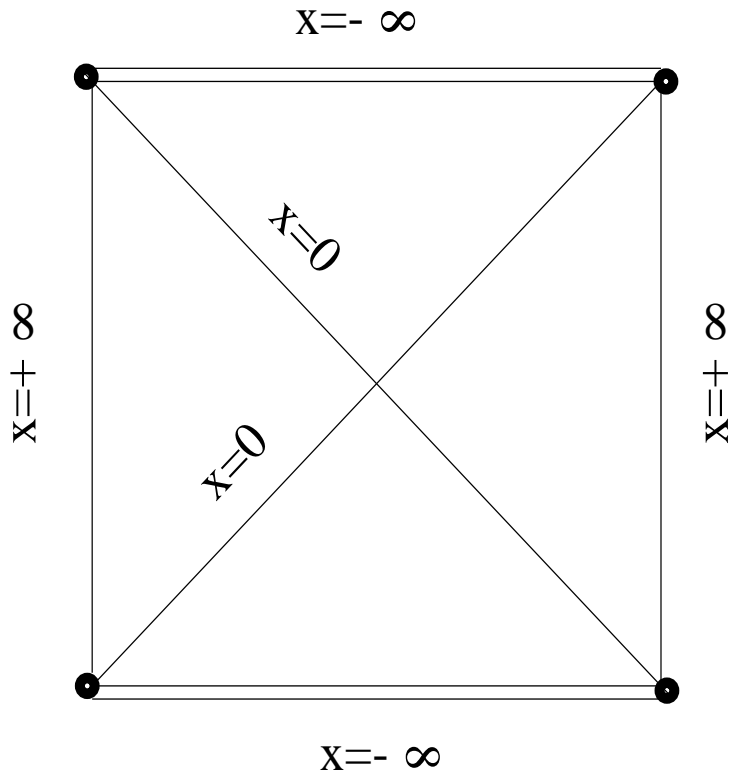


Fig. 5: Penrose diagram for the first-class black hole with n odd.

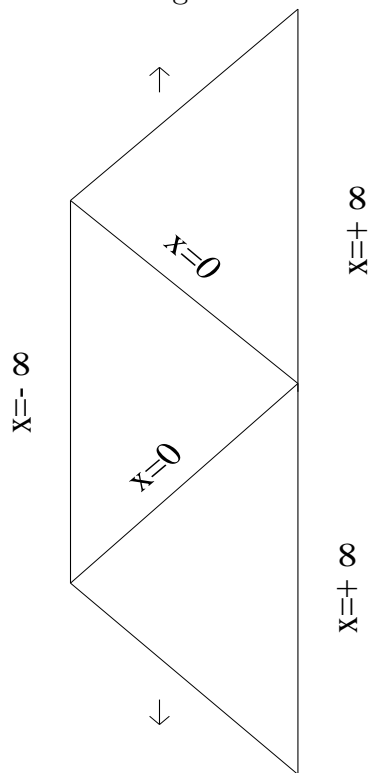


Fig. 6: Penrose diagram for the first-class black hole with n even.

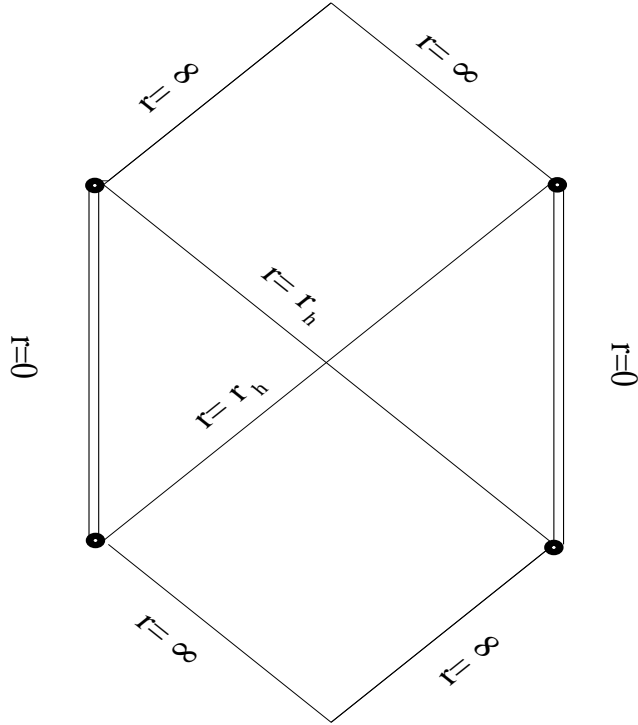


Fig. 7: Penrose diagram for the spacetime (4.14)-(4.15) with $\kappa > 0$.

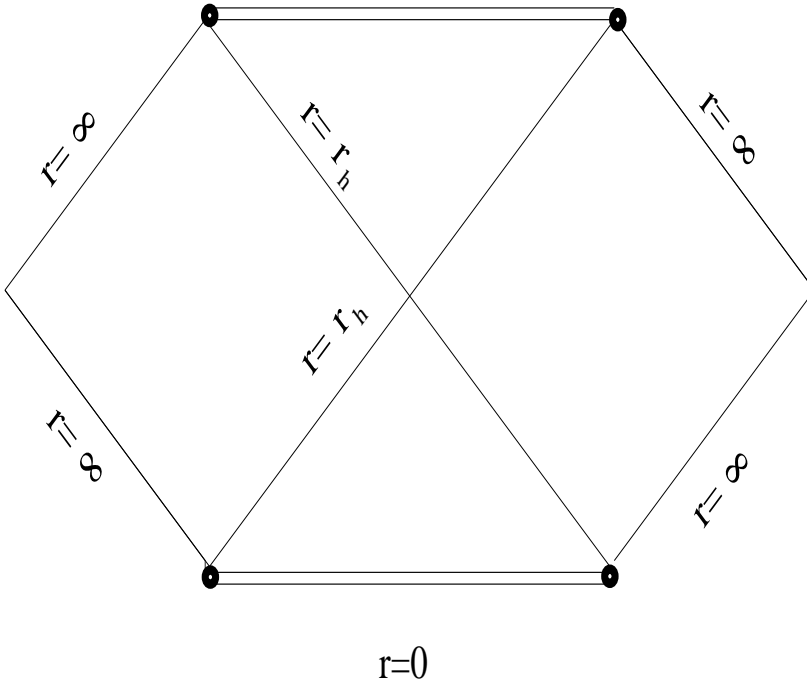


Fig. 8: Penrose diagram for the second-class black hole (spacetime (4.14)-(4.15) with $\kappa < 0$).

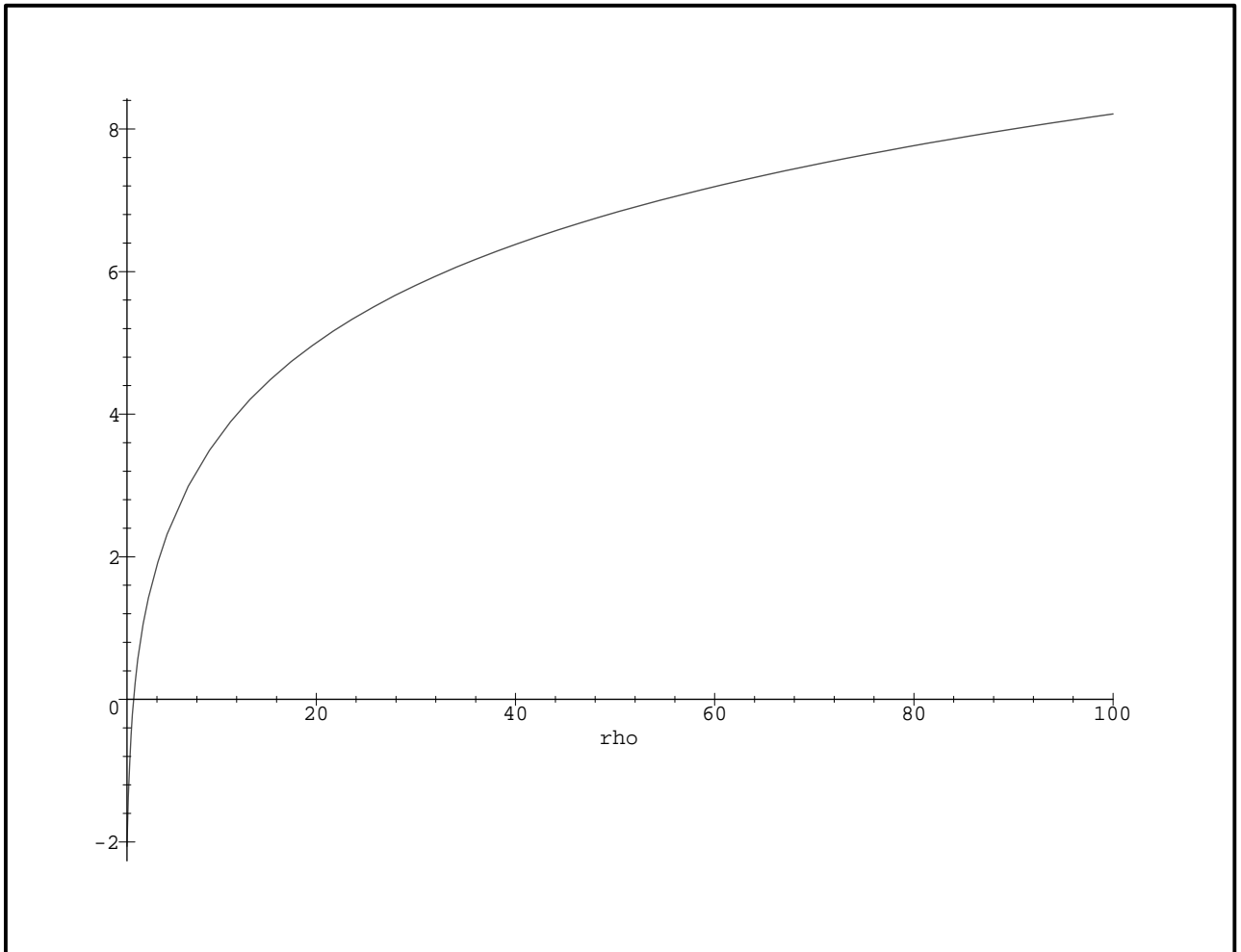


Fig. 9: Graph of the potential $V(\rho)$ (Eq. (4.17)) for $\epsilon = +1$, $B = 1$ and $\lambda = 1$.

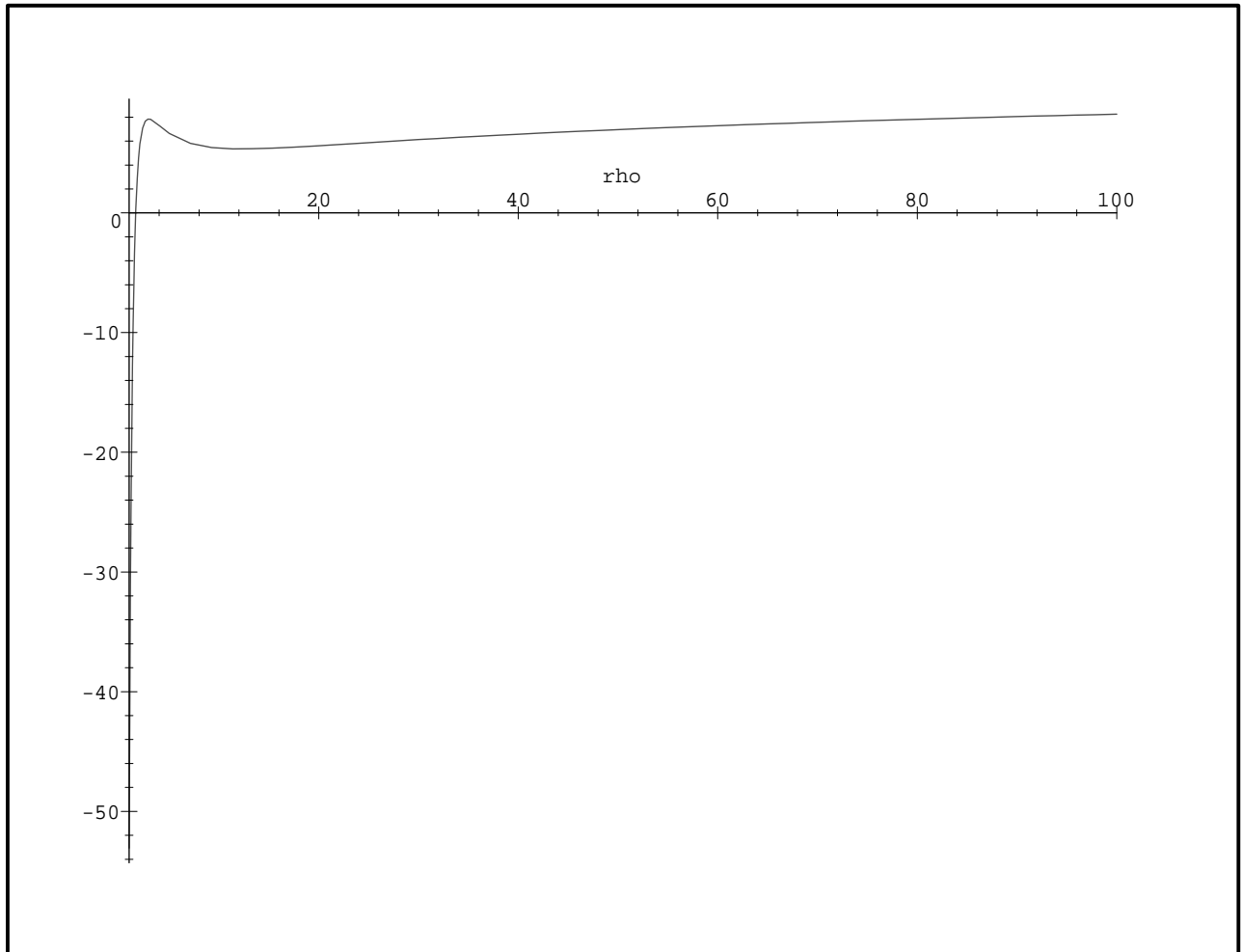


Fig. 10: Graph of $V(\rho)$ for $\epsilon = +1$, $B = 1$ and $\lambda = 50$ (case $\lambda > e^{1+\frac{B}{2}}$).